Int. J. Electrochem. Sci., 14 **(2019)** 5287 – 5304, doi: 10.20964/2019.06.63

International Journal of ELECTROCHEMICAL SCIENCE
www.electrochemsci.org

Mini review

Metal-Organic Frameworks-Based Electrochemical Sensors and Biosensors

Feng Zhao, Ting Sun[*]*, Fengyun Geng, Peiyu Chen and Yanping Gao*[*]

College of Chemistry and Chemical Engineering, Anyang Normal University, Anyang, Henan 455000, People's Republic of China
[*]E-mail: tingsunhx@aliyun.com; fygu2010@163.com

Received: 9 March 2019 / *Accepted:* 11 April 2019 / *Published:* 10 May 2019

Metal–organic frameworks (MOFs) exhibit distinguish properties, including permanent porosity, abundant structures and tailorable surface chemistry. Recently, MOFs have been widely used in the electrochemical sensing fields as the electroactive materials or signal labels. This review focuses on the recent progress in the development of MOFs-based electrochemical sensors and biosensors.

Keywords: Metal-organic frameworks; electrochemical biosensors; signal labels

1. INTRODUCTION

Metal-organic frameworks (MOFs), formed by organic ligand and metal ions or clusters *via* strong coordination bonds, are a promising class of crystalline porous materials due to their distinguish properties, such as permanent porosity, abundant structures and tailorable surface chemistry. MOFs have offered a wide range of applications in catalysis, energy, separation, gas storage, biomedical imaging, drug delivery and so forth [1-3]. Recently, numerous research groups have putted increasing attentions to explore the application of MOFs as sensing materials, including optical, electrochemical, mechanical, and photoelectrochemical sensors, categorized by signal transduction [4, 5]. Particularly, the utilization of MOFs as the signal labels of electrochemical sensors is one of their most important and potential applications. Some of MOFs exhibit good electrochemical activity and cab be employed to develop novel electrochemical sensors if metal ions and organic linkers of MOFs are well designed. Meanwhile, MOFs with high specific surface areas and exposed active sites can possess the superior enzyme-like catalytic activity for a range of substrates, which endows them with the potential to being used as nanozymes to construct different types of sensors. For example, Cu-based MOFs have been

reported to have intrinsic peroxidase-like activity for the catalytic oxidation of TMB in the presence of H_2O_2 [6]. Although a lot of papers involving in MOFs-based sensors have been published, electrochemical applications of MOFs as the signal labels are still limited because of their weak electronic conductivity and electrocatalytic ability.

In view of the rapid development of nanoscience, in the past decades, the developments and innovations in preparation and assembly of nanomaterials have opened numerous opportunities for improving the performance of MOFs in electrochemical-related field. Different hybrids have been synthesized by integrating other functional guest molecules or nanomaterials into MOFs [7]. Among those preeminent hybrids, the combination of MOFs and carbon nanomaterials, such as carbon nanotubes (CNTs) and graphene oxide (GO), can dramatically improve the electrical conductivity and mechanical strength of the nanocomposites. On the other hand, the challenges lay in the low catalytic activity of MOFs could also be overcome by assembling catalytically active guest materials into MOFs. For example, metal nanoparticles (NPs) including palladium, gold, copper, and ruthenium have been used to decorate MOFs for an increased catalytic efficiency.

This review highlights the recent developments in MOFs as electrochemical sensors and biosensors. First, we briefly summarize the application of some MOFs as the electrochemical materials for electrocatalysis. Then, we mainly focus on the design of MOFs as the signal labels, in which MOFs can be used as electrocatalytic labels for signal amplification and as carriers for metal ions and functional biomolecules (DNA, aptamers, antibody and enzymes).

2. MOFS AS THE ELECTROCHEMCIAL MATERIALS FOR ELECTROCATALYSIS

In general, the metal ions or clusters of inorganic nodes in MOFs can exhibit electrocatalytic oxidation/reduction ability toward various molecules. The functional groups in organic linkers can adsorb targets of interest as preconcentration for further electrocatalysis. To date, plenty of molecules have been efficiently determined by directly using MOFs as electrocatalytic electrode materials, including hydrogen peroxide, nitrite, metal ions, glucose and other small organic molecules. The analytical performances are listed in Table 1.

H_2O_2 detection has attracted worldly attention due to its wide applications in fuel cells, pharmaceutical industry, food industry, and environmental protection. It is well known that H_2O_2 undergoes electrochemical oxidation or reduction processes at solid electrodes. Since Cu-MOFs were used as electrocatalysts for H_2O_2 oxidation, a few of nonenzymatic electrochemical sensors for H_2O_2 have been developed and investigated based on different MOFs [8-11]. To improve the electrocatalytic ability toward H_2O_2 oxidation or reduction, many nanocomposites, including MOF's derivates and hybrids with nanomaterials or proteins, have been prepared and used to detect H_2O_2 [12-17]. For example, Xu and co-workers demonstrated that UiO-66 encapsulated with platinum nanoparticles (Pt NPs) can be used for nonenzymatic detection of H_2O_2 [14].

Accurate, rapid, and sensitive detection of nitrite (a well-known preserving agent and biomarker in the food and health industries) have attracted much attention. Zirconium-based porphyrin MOF (MOF-525) and Pd/NH_2-MIL-101(Cr) have been demonstrated to exhibit good electrocatalytic activity for nitrite oxidation [18, 19]. Moreover, Au microspheres on Cu-MOFs could further decrease

the oxidation potential by accelerating the electron transfer rate of electro-oxidation of nitrite.

Heavy metal ions have been widely recognized as hazardous factors to environment and human, and could be detected by anodic stripping voltammetry. Due to the large surface area and tunable chemical functionality, MOFs and their hybrids can be used to modify the electrode, in which the composite can adsorb metal ions via the interaction between hydrophilic groups and metal cations and thus enhance the performance of the electrode [20-23]. Wang and co-workers reported that UiO-66-NH_2 prepared by in situ growth with graphene aerogels (GA) as the backbone can be modified on the glassy carbon electrode (GCE) for simultaneous detection of multiple heavy-metal ions [23].

In 2013, Mao's group firstly demonstrated that ZIFs can serve as the matrix for co-immobilization of methylene green (MG) (a redox active dye) and glucose dehydrogenase (GDH) (a dehydrogenase) onto the electrode surface for sensitive detection of glucose with a linear range of 0.1 ~ 2 mM [24]. After that, FeTCPP-modified porous carbon derived from ZIF-8 and AgNPs@Zn-MOF modified with glucose oxidase were employed to construct sensitive electrochemical biosensors for glucose [25, 26] . However, all the above sensors require the use of glucose oxidase, which is unstable in detection environments and storage environments. Therefore, non-enzymatic electrocatalytic oxidation of glucose sensors are developed by researchers based on MOFs and their derivates, especially Ni- and Cu-MOFs [27-29].

Table 1. Analytical performances of MOFs-modified electrodes for biosensing

Analytes	Electrode Materials	Linear ranges	Detection limits	Refs.
H_2O_2	[Cu(adp)(BIB)(H_2O)]n	0.1 ~ 2.75 μM	0.068 μM	[8]
	[Co(pbda)(4,4-bpy)·2H_2O]n	0.05 ~ 9.0 mM	3.76 μM	[9]
	MIL-53-Cr^{III}	25 ~ 500 μM	3.52 μM	[10]
	AP-Ni-MOF	0.004 ~ 60 mM	0.9 μM	[11]
	Cu-MOF loaded on macroporous carbon	10 ~ 11600 μM	3.2 μM	[12]
	Pt NPs@UiO-66 (core−shell heterostructure)	0.005 ~ 14.75 mM	3.06 μM	[14]
	Cu-TDPAT modified with nanosized electrochemically reduced graphene oxide	4 ~ 12 000 μM	0.17 μM	[15]
	mesoZIF-8 encapsulating cytochrome *c*	0.09 ~ 3.6 mM	Not reported	[16]
	MOF-derived Fe_2O_3 nanoparticle	3 ~ 150 μM 150 to 750 μM	0.17 μM	[17]
Nitrite	MOF-525	20 ~ 800 μM	2.1 μM	[18]
	Pd/NH_2-MIL-101(Cr)	5 ~ 150 nM	1.3 nM	[19]
Metal ions	MOF-5 [$Zn_4O(BDC)_3$]	0.01 ~ 8 μM (Pb^{2+})	4.9 nM	[20]
	[$H_2N(CH_3)_2]_4[Zn_3(Hdpa)_2]$·4DMF	5 pM ~ 0.9 μM (Cu^{2+})	1 pM	[21]
	Ni-MOF	500 nM ~ 6 μM (Pb^{2+})	508 nM	[22]

		graphene aerogel@UiO-66-NH_2	0.06 ~ 3 μM (Cd^{2+}) 0.01 ~ 4 μM (Pb^{2+}) 0.1 ~ 3.5 μM (Cu^{2+}) 0.005 ~ 3 μM (Hg^{2+})	0.02 μM 1.5 nM 7 nM 2 nM	[23]
Glucose		Ni/NiO/carbon frame/Ni-MOF	4 ~ 5664 μM	0.8 μM	[27]
		Ni-MIL-77 nanobelts	1 ~ 500 μM	0.25 μM	[28]
		AgNPs/ZIF-67	2 ~ 1000 μM	0.66 μM	[29]
		Cu-MOF	0.002 ~ 1.4 mM 1.4 ~ 4.0 mM	0.6 μM	[30]
		MOF-Derived Porous Ni_2P/Graphene	0.005 ~ 1.4 mM	0.44 μM	[31]
		Co-MOF on Ni foam	0.001 ~ 3 mM	1.3 nM	[32]
		NiCo-MOF nanosheets array	0.001 ~ 8 mM	0.29 μM	[33]
	AP	Ferrocene-immobilized in-MOF	0.01 ~ 20 μM	6.4 nM	[34]
		Cu-MOF modified with electrochemically reduced graphene	1 ~ 100 μM	0.36 μM	[35]
	DA	MIL-101	5 ~ 250 μM	Not reported	[36]
		Cu-MOF modified with electrochemically reduced graphene	1 ~ 50 μM	0.21 μM	[35]
		C/Al-MIL-53-$(OH)_2$	0.03 ~ 10 μM	8 nM	[37]
		Mn-MOF@MWCNT	0.01 ~ 500 μM	0.002 μM	[38]
		ZIF-8@graphene	0.003 ~ 1 mM	1 μM	[39]
	UA	MIL-101	30 ~ 200 μM	Not reported	[36]
		Mn-MOF@MWCNT	0.02 ~ 1100 μM	0.005 μM	[38]
Small organic molecules	AA	$[Cu_2(HL)_2(\mu_2\text{-}OH)_2(H_2O)_5]$ H_2O_n	0.25 ~ 1.5 mM	Not reported	[40]
		Mn-MOF@MWCNT	0.1 ~ 1150 μM	0.01 μM	[38]
	H	Au-SH-SiO_2@Cu-MOF	0.04 ~ 500 μM	0.01 μM	[41]
	Cys	Au-SH-SiO_2@Cu-MOF	0.02 ~ 300 μM	0.008 μM	[42]
	HQ	Cu-MOF-199@SWCNT	0.1 ~ 1453 μM 0.1 ~ 1150 μM	0.08 μM 0.1 μM	[43]
	DHA	$Cu_3(BTC)_2$	0.04 ~ 1 μM	9 nM	[44]
	HA	AuNPs/MMPF-6(Fe)	0.01 ~ 1 μM and 1 ~ 20 μM	0.004 μM	[45]
	urea	Ni-MOF@MWCNT	0.01 ~ 1,12 mM	2.5 μM	[46]
	ATP	Cu-MOF@ electroreduced graphene oxide	0.2 ~ 10 μM	0.1 μM	[47]
	BPA	CTAB/Ce-MOF	0.005 ~ 50 μM	2 nM	[48]
	GA	Mo_xC@C derived from polyoxometalates@Cu-MOF	0.03 ~ 122 μM 0.02 ~ 122 μM	8.5 nM 8.0 nM	[49]

Abbreviations: BIB: 1,4-bisimidazolebenzene; adp: adipic acid; 4,4-bpy: 4,4-bipyridine; pbda: 3-(pyridine-3-yloxy)benzene-1,2-dicarboxylic acid; AP: adipic acid; TDPAT: 2,4,6-tris(3,5-dicarboxylphenylamino)-1,3,5-triazine; DMF: dimethylformamide; Hdpa: 3,4-di(3,5-dicarboxyphenyl)phthalic acid; MWCNT: multi-walled carbon nanotubes; H_2L: 2,5-dicarboxylic acid-

3,4-ethylene dioxythiophene; SWCNT: single-walled carbon nanotubes; H_3BTC: 1,3,5-benzenetricarboxylic acid; CTAB: hexadecyl trimethyl ammonium bromide.

Small organic molecules can be directly detected by electrochemical methods based on the electrochemical oxidation or reduction. However, they often suffer from weak anti-interference ability, poor sensitivity and selectivity due to the low electrocatalytic activity and capacity. This can be resolved by using MOFs as electrocatalytic electrochemical materials. In most cases, MOFs can not only provide a lot of electroactive sites to lower the energy barrier for oxidation or reduction, but also can promote the electron/proton transfer between molecules and the electrode. Besides, MOFs can adsorb organic molecules through strong π-π, charge donor–acceptor and electrostatic interactions between molecules and organic linkers. The analytical performances of MOFs-modified electrodes for the detection of small organic molecules have also presented in Table 1, including acetaminophen (AP), dopamine (DA), uric acid (UA), ascorbic acid (A)A, hydrazine (H), cysteine (Cys), hydroquinone catechol (HQ), 2,4-dichlorophenol hydroxylamine (DHA), 2,4,6-trinitrophenol (ATP), bisphenol A (BPA), and guanine adenine (GA).

3. MOFS AS THE ELECTROCHEMCIAL SIGNAL LABELS

Due to large surface area and manipulatable structural properties, MOF is a promising type of signal probe for constructing electrochemical biosensors. For example, MOFs with electrocatalytic ability toward redox substrates as well as electroactive properties from redox-active ligands or metal nodes and MOFs loading with electroactive molecules or ions have been extensively used to design electrochemical biosensing methods. Besides, biomolecules can be modified on the surface of MOFs to regulate the access of redox molecules in solution to the surface of electrodes as gate, which can be sensitively monitored by electrochemical impedance spectroscopy.

2.1 MOFs as electrocatalysts

As the active center of natural enzymes, porphyrins and its derivates have been widely applied as mimetic molecules to catalyze organic reactions, such as olefin epoxidation and epoxidation of hydrocarbons [50-52]. Recently, porphyrin-based MOFs are reported to possess peroxidase-like catalytic activity and employed to develop fluorescence, colorimetric and electrochemical biosensors [53, 54]. Lei's group reported the "signal-on" electrochemical detection of DNA using a prototypal MOF of HKUST-1(Cu) encapsulated with one-pot synthesized iron(III) meso-5,10,15,20-tetrakis(4-carboxyphenyl) porphyrin chloride (FeTCPP) as mimetic catalysts (Figure 1A) [55]. The addition of target DNA triggered the allosteric switch of hairpin DNA to activate SA aptamer. Then, the specific recognition between SA and its aptamer can introduced FeTCPP@MOF-SA probe to the electrode surface. The nanoprobe can significantly catalyze the oxidation of *o*-phenylenediamine (o-PD) to 2,2'-diaminoazobenzene in the presence of H_2O_2 and generate a typical electrochemical signal. This elaborate sensor had a wide linear range of 10 fM to 10 nM with a detection limit lower to 0.48 fM. Lei and co-workers further designed a nanoscaled porphyrinic MOF (PorMOF) for electrochemical

detection of telomerase activity, in which iron porphyrin and zirconium ion were used as the linker and the node, respectively (Figure 1B) [56]**.** Once telomerase triggered the extension of the assistant DNA 1 (aDNA1) in duplex in the presence of dNTP mixture, the assistant DNA 2 (aDNA2) was liberated and subsequently hybridized with the capture DNA (cDNA), and the streptavidin (SA) conjugated PorMOF was introduced to the electrode surface with the biotin-streptavidin biorecognition, resulting in an increased current of electrocatalytic O_2 reduction. The designed sensor exhibited high stability in broad conditions and even could detect the telomerase activity in a single HeLa cancer cell (2.2×10^{-11} IU). They also applied another type of PorMOFs (PCN-222) as signal nanoprobes for sensitive detection of DNA with the aid of triple-helix molecular switch and DNA recycling amplification of Exonuclease III [57]. Moreover, Ju's group prepared iron-porphyrinic metal-organic framework ((Fe-P)$_n$-MOF) without other metal ions and modified with Au nanoparticles (AuNPs) to anchor DNAzyme, GR-5 (Figure 1C) [58]. Under the addition of Pb^{2+}, GR-5 could be specifically cleaved at the ribonucleotide (rA) site and the produced (Fe-P)$_n$-MOF-labeled short DNA further hybridized with HP bound on the surface of screen-printed carbon electrode (SPCE). The peroxidase-like (Fe-P)$_n$-MOF could catalyze the oxidation of TMB by H_2O_2, significantly increasing the reduction peak current. This endows the SPCE-based assay with the potential application for low-cost and on-site Pb^{2+} detection in various environments.

According to the previous works, Cu-MOFs can also possess superior catalytic activity towards various substrates and have be widely used in constructing diverse biosensors for the detection of interests. Yuan's group developed a sensitive and accurate electrochemical biosensor for lipopolysaccharide (LPS), integrating the superior catalytic ability of Cu-MOFs and the quadratic signal amplification of target protein (Figure 1D) [59]. They prepared Cu-MOFs via a hydrothermal method and *in situ* generated AuNPs on the surface of Cu-MOFs to carry hairpin probes 3 (HP3/AuNPs/Cu-MOFs). Upon the addition of LPS, the cycle I was initiated with the aid of phi29 and a lot of output DNA were produced, which could trigger the N.BstNBI-mediated cyclic hairpin assembly (cycle II), leading to the broken of ferrocene-labeled hairpin probes 2 (Fc-HP2) and the production of a large amount of capture probes. When the hybridization of capture probes and HP3/AuNPs/Cu-MOFs, large amounts of Fc left from the electrode and large amounts of HP3/AuNPs/Cu-MOFs are brought to the surface. Since Cu-MOFs catalyzed the oxidation of glucose to gluconolactone for the enzyme-free third signal amplification, the change of Fc number and Cu-MOFs would lead to the remarkable ratiometric electrochemical response. In view of the merits of the ratiometric electrochemical assays, this strategy decreased the difference between different patches and has great potential in other analytes detection in complex samples.

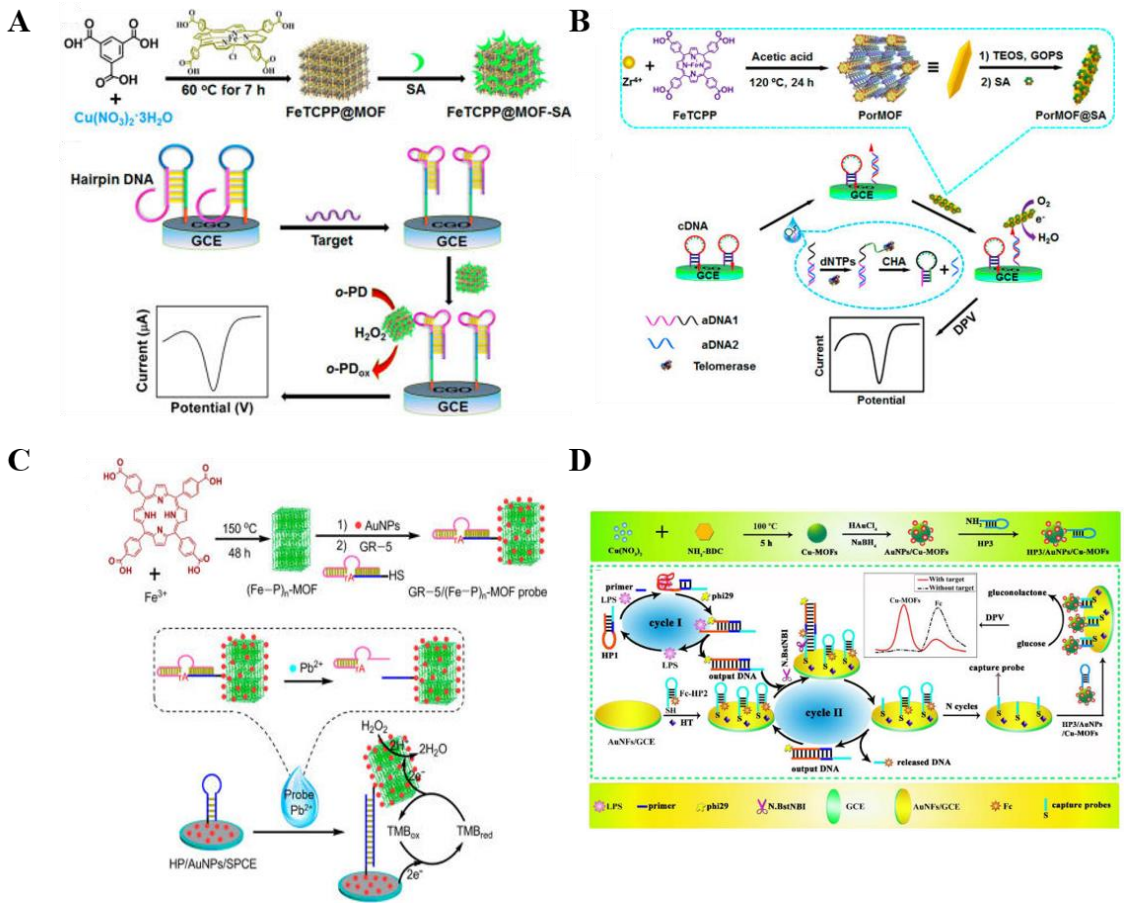

Figure 1. (A) Synthesis of FeTCPP@MOF-SA composite and electrochemical DNA sensing via allosteric switch of hairpin DNA. Reprinted with permission from [55]. Copyright 2015 American Chemical Society. (B) Schematic illustration of the preparation of nanoscaled PorMOF and the electrochemical detection strategy for telomerase activity via a telomerase triggered conformation switch. Reprinted with permission from [56]. Copyright 2016 American Chemical Society. (C) Schematic representation of preparation of GR-5/(Fe-P)$_n$-MOF probe and electrochemical detection of Pb^{2+}. Reprinted with permission from [58]. Copyright 2015 American Chemical Society. (D) Schematic illustration of the fabrication of the aptasensor: preparation procedure of HP3/AuNPs/Cu-MOFs and signal amplification strategy and the detection principle for LPS. Reprinted with permission from [59]. Copyright 2015 American Chemical Society.

Other MOFs, containing metal ions with mixed valence state or multiple valence state, can also possess enzyme-like catalytic ability, and have been used in colorimetric and electrochemical detection. Chen's group has reported that three distinct structures of Co/Fe-based MOFs and mixed valence state Ce(III, IV)-MOF have intrinsic catalytic activities towards the electrochemical reduction of thionine (Thi, a dye molecule) without any substrates (*i.e.* H_2O_2). The MOFs have been applied to sensitively detect thrombin and ochratoxin A [60, 61]. Besides, MOFs with redox-active ligands can also be used as electroactive nanoprobes without the addition of any redox mediators. Based on this principle, Chen's group designed an electroactive MOF (Ni-MOF) with 4,4',4''-tricarboxytriphenylamine as the electroactive source and Ni_4O_4 cluster as the node. The resulting Ni-MOF was applied for electrochemical aptasensing of thrombin [62].

Moreover, noble-metal NPs or alloy NPs not only can be absorbed on the surface of MOFs to anchor recognition unites and enhance electric conductivity, but also can be employed as nanozymes with fascinating catalytic activities [63]. Yuan's group decorated electroactive Co-based MOFs with HRP-like PtPd NPs and DNA HP3 as a redox mediator (Co-MOFs/PtPdNPs/HP3). The MOFs were used for the detection of thrombin (TB) based on the strategy of target-triggering nicking enzyme signaling amplification (NESA) with the aid of nicking endonuclease (Nt.AlwI) (Figure 2A) [64]. Unlike traditional NESA strategy, in this work, all the produced DNA fragments from the repeated cycles of hybridization-cleavage initiated by the recognition between TB and the corresponding aptamer could unfold the DNA HP2 to bring Co-MOFs/PtPdNPs/HP3 close to the surface of the electrode. In the presence of H_2O_2, PtPd NPs catalyzed the oxidation of H_2O_2 and promoted the conversion of Co^{2+} to Co^{3+}, further leading to the improvement of the characteristic electrochemical signal. This aptasensor showed good selectivity, stability and high sensitivity from 1 pM to 30 nM. The group also prepared hemin-encapsulated Fe-MOFs/PtNPs composites via a one-pot reduction. The electrocatalytic nanoprobes have the synergistic catalytic activity toward H_2O_2 by hemin and PtNPs, and have been used to electrochemical detection of cell-free fetal DNA (cffDNA) [65]. Recently, electrocatalytic MOFs were combined with DNA-walker-induced conformation switch for ultrasensitive detection of target DNA (Figure 2B) [66]. First, porphyrinic MOFs (PCN-224) were modified with palladium nanoparticles (Pd NPs) via in situ reduction and then conjugated with SA as a recognition element (Pd/PCN-224-SA).

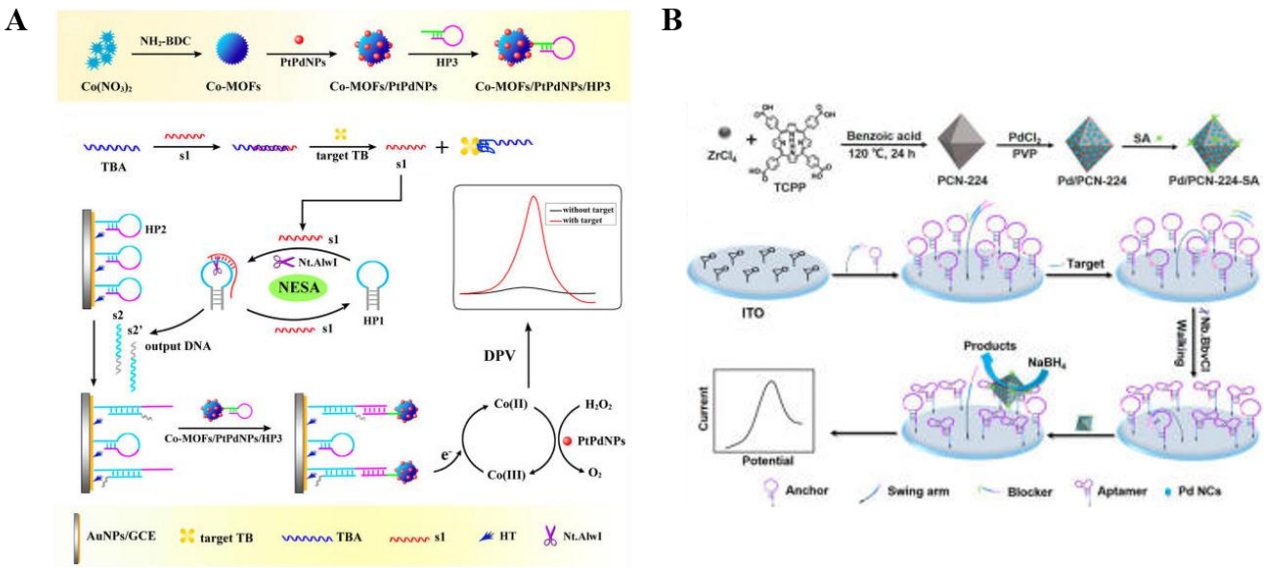

Figure 2. (A) Schematic illustration of the preparation of the preparation of Co-MOFs/PtPdNPs/HP3and the detection principle for TB. Reprinted with permission from [64]. Copyright 2017 American Chemical Society. (B) Schematic illustration of the synthesis of Pd/PCN-224-SA tags and the tandem signal amplification strategy based on DNA-walker-induced allosteric switch and electrocatalysis of Pd/PCN-224-SA in electrochemical biosensing. Reprinted with permission from [66]. Copyright 2018 American Chemical Society.

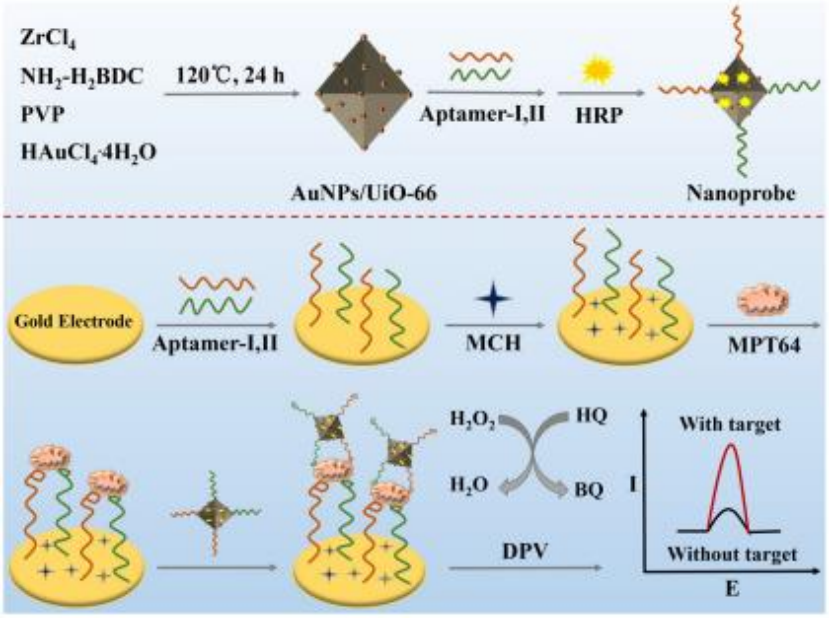

Figure 3. Schematic illustration of the process of the fabrication of the aptamer/HRP/ AuNPs/UiO-66-NH_2 nanoprobes and the electrochemical aptasensor. Reprinted with permission from [67]. Copyright 2018 Springer Nature.

Then, they immobilized the DNA walker substrate on the surface of the indium tin oxide (ITO) electrode, consisting of a SA aptamer sequence as the track and blocked swing arm as the walker strand. The added target DNA can hybridize with the blocker through a strand-displacement reaction, leading to swing arms away from the blocker. Thus, the autonomous moving of DNA walkers was activated and further powered by the nicking endonuclease (Nb·BbvCI)-catalyzed cleavage of hairpin DNA. The produced DNA changed to SA aptamer and brought Pd/PCN-224-SA to the electrode surface via the SA-aptamer recognition, resulting in the enhanced electrochemical signal. This DNA walker-based system has the advantages of a wide detection linear range, low LOD and single-base mismatch discrimination ability.

Due to the tunable chemical functionality and porous structures, MOFs have been used to load drug, protein, and enzyme for the biomedical applications [68-70]. For example, horseradish peroxidase (HRP) can catalyze the oxidation of substrates by H_2O_2, and has been encapsulated into MOFs as electrocatalysts. Chen's group prepared two aptamers-conjugated Zr(IV)-based MOF (UiO-66-NH_2) to carry HRP for the detection of the *Mycobacterium tuberculosis* antigen MPT64 (Figure 3) [67]. In the assay, the surface of MOF was decorated with AuNPs by a one-step hydrothermal synthesis. The surface of gold electrode and AuNPs/MOF both were labeled with two aptamers with synergistic effect on binding MPT64. This assay showed a wide linear range from 0.02 to 10000 pg mL^{-1} and a lower detection limit (10 pg mL^{-1}). Ai's group used zeolitic imidazolate framework to load secondary antibodies (Ab_2) and HRP for signal amplification detection of avian leukosis virus subgroup J [71].

2.2 Carriers for metal ions

According to previous reports, metal ions, including Cd^{2+}, Pb^{2+}, Cu^{2+} and Zn^{2+}, exhibit typical voltammetric characteristics at different applied potentials and have been employed as electroactive indicators for electrochemical bioassays of metal ions or other molecules [72-82]. For example, Li's group utilized Cu^{2+} ions as the signal-generation indicators to construct a direct electrochemical method for ultra-trace Cu^{2+} [73]. Normally, to provide high electrochemical signals, metal ions should be doped into NPs via ions exchange or be encapsulated into the dendrimer as signal unit [83-85]. However, the modification processes were sometimes time-consuming.

Because of the special pore structure, high surface area, large amounts of metal ions as the nodes and abundant functional groups in sidewalls, MOFs have also been employed to carry different electroactive metal ions to develop electrochemical biosensors. For instance, Chen and co-workers employed UiO-66-NH_2 as substrate to carry different metal ions (Cd^{2+} and Pb^{2+}) for simultaneous detection of multiple antibiotics based on the specific biorecognition between the corresponding aptamers and antibiotics [86]. Recently, Zhao's group also utilized the same strategy for simultaneous electrochemical immunosensing of triazophos (TRS) and thiacloprid (THD), displacing DNA with antigen and antibody (Figure 4) [87]. In this study, UiO-66-NH_2 was used to adsorb large amounts of Cd(II) and Pb(II) ions with amino functional groups on the surface, in which the adsorption capacities were 230 and 271 $mg \cdot g^{-1}$, respectively. Next, ions-loaded UiO-66-NH_2 were labeled with TRS or THD Ag as the signal tags and carboxyl functionalized magnetic bead (MB-COOH) were coupled with TRS or THD Ab as the capture probes. In the presence of TRS and THD, the matching MOFs are specifically replaced and released into the supernatant. After magnetic separation, the dual peak currents of Cd^{2+} and Pb^{2+} in the supernatant are observed simultaneously in one cycle of SWV.

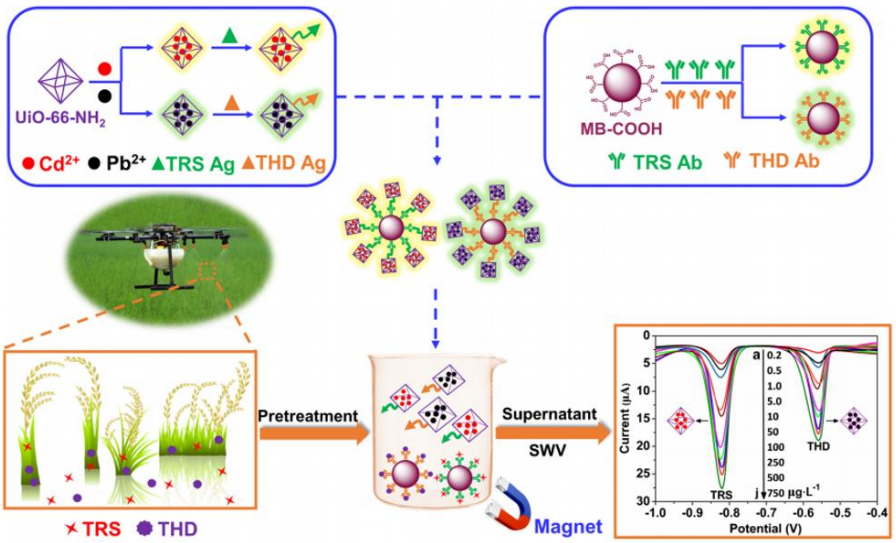

Figure 4. Schematic presentation of an amino-modified metal-organic framework (type UiO-66-NH_2) loaded with Cd(II) and Pb(II) ions for simultaneous electrochemical immunosensing of triazophos (TRS) and thiacloprid (THD).. Reprinted with permission from [87]. Copyright 2019 Springer-Verlag.

Unlike traditional signal probes adsorbing additional electroactive metal ions on the surface of MOFs, Yang's group first demonstrated that Cu^{2+}-based MOFs (HKUST-1) alone were directly used as electrochemical signal probes, and Cu^{2+} in HKUST-1 was directly detected by differential pulse voltammetric (DPV) scan (Figure 5A) [88]. This circumvents the limitation of acid dissolution and preconcentration. To rule out the possibility of electrochemical signal derived from free ions adsorbed on MOFs, the authors conducted a series of experiments and characterization. Furthermore, covalent organic frameworks (COFs) modified with Pt NPs as the substrate to immobilize capture antibodies and improve the electronic conductivity. After the formation of the immunocomplex, a high electrochemical signal could be detected due to large amounts of Cu^{2+} in HKUST-1. Under the optimized paraments, this electrochemical immunoassay showed an excellent analytical performance for C-reactive protein (CRP) detection and had a linear dynamic ranging from 1 to 400 ng/mL with a detection limit of 0.2 ng/mL. Moreover, they found that other metal ion-contained MOFs (such as Cd^{2+}- or Zn^{2+}- based MOFs) can also be employed as electroactive signal probes for bioanalysis. In contrast, Ma's group successfully prepared two aminated MOFs (Pb-BDC-NH_2 and Cd-BDC-NH_2) from Pb(II) or Cd(II) and 2-aminoterephthalic acid (BDC-NH_2) and decorated them with two different antibody toward carcinoembryonic antigen (CEA) and alpha-fetoprotein (AFP) for immunosensoring (Figure 5B) [89]. After the formation of immunocomplex in 48-well plate, the bound MOFs were dissolved by nitric acid. Two liberated metal ions could be easily detected at voltages of −0.63 and −0.88 V by polyaniline (PANI) nanofibers modified glassy carbon electrode (GCE), respectively. The presence of PANI improved the electronic conductivity of electrode and the chemical polymerization method enhanced the accuracy and reproducibility of results.

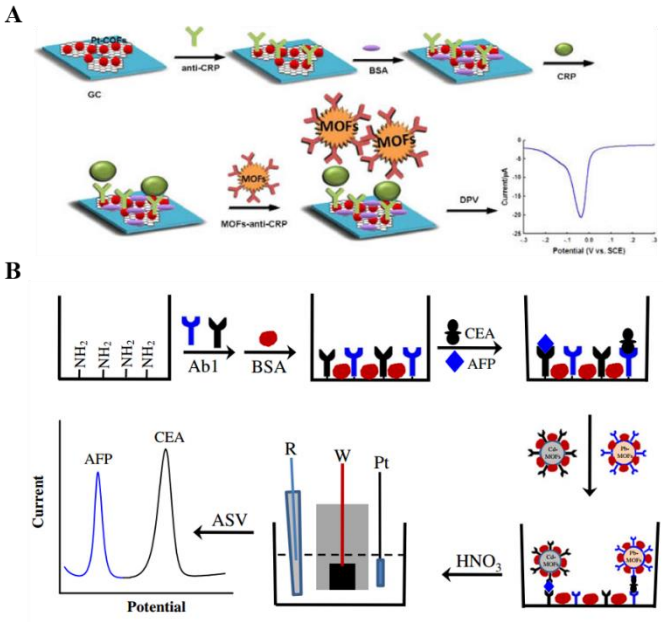

Figure 5. (A) Schematic illustration of the electrochemical immunosensor for CRP based on Cu-MOFs. Reprinted with permission from [88]. Copyright 2016 American Chemical Society. (B) Schematic illustration of the stepwise immunoanalysis process for CEA and AFP based on two MOFs. Reprinted with permission from [89]. Copyright 2017 Springer-Verlag.

2.4 Small molecules

Functional biomolecules (e.g. DNA, aptamer, antibody and enzyme) can specifically react with target molecules, and thus have been widely utilized in developing biosensors, including fluorescence, colorimetric, electrochemiluminescence and electrochemical biosensors [90-92]. In MOFs-based electrochemical biosensors, MOFs with pendent functional groups (such as -NH_2 and -COOH) can couple with those biomolecules. Sometimes, organic ligands in MOFs usually having π-electron systems and special functional groups can strongly adsorb single-stranded DNA (ssDNA) in the interior and on the surface of porous MOFs through π–π stacking, hydrogen-bonding, and electrostatic interactions. Meanwhile, Zr-based MOFs can also possess high affinity toward biomolecules containing phosphate groups through the covalent bonds between Zr ion and phosphate radical [93, 94].

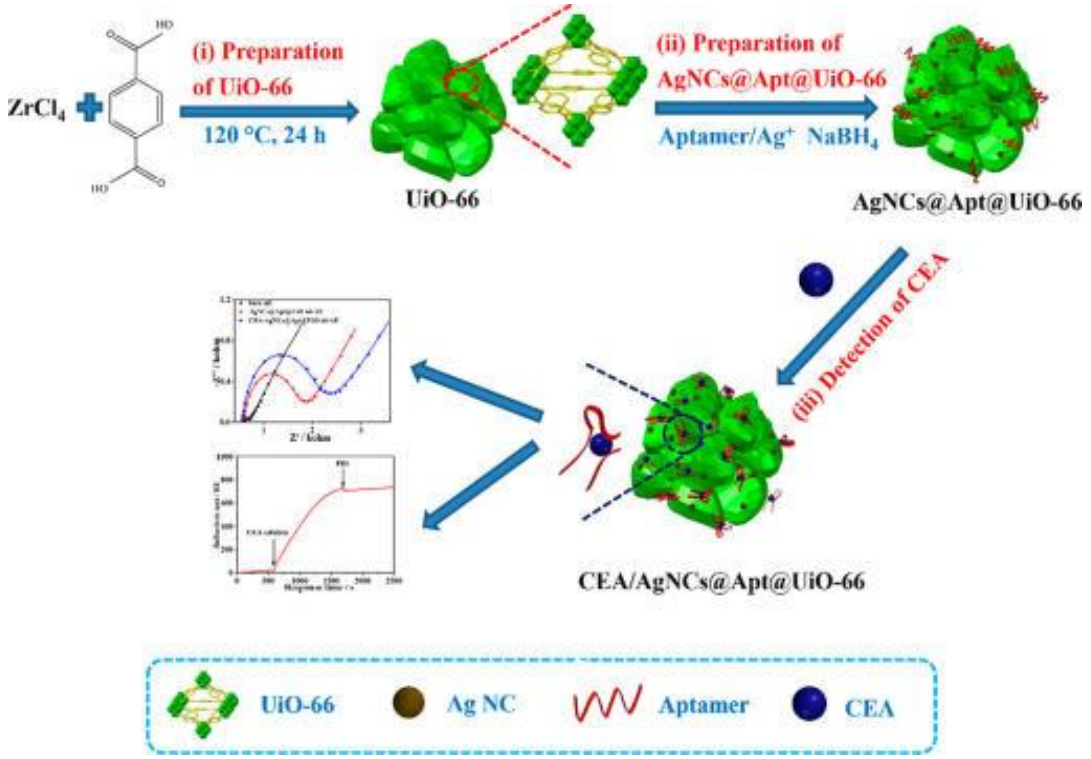

Figure 6. Schematic diagram of the AgNCs@Apt@UiO-66-based aptasensor for detecting CEA. Reprinted with permission from [99]. Copyright 2017 American Chemical Society.

In an electrochemical aptasensor, the adsorption of aptamer and the target-induced change of the structure or configuration of DNA will subsequently have a significant influence on the electron transfer between the electrode and the electrolyte solution, which is always evaluated by electrochemical impedance spectroscopy. Based on this strategy, a few of MOFs and their derivates have been employed to develop non-label aptasensors for the detection of various molecules, including antibiotics [95], drug [96], heavy metal ions (Pb^{2+} and As^{3+}) [97] and proteins [98-100]. For instance, Du's group successfully synthesized three Zr-MOFs with different terminal ligands in channels and employed them to anchor aptamer strands for constructing electrochemical aptasensor for lysozyme

detection [98]. At the same time, Zhang's group also reported a bifunctional electrochemical and surface plasmon resonance (SPR) aptasensor for carcinoembryonic antigen (CEA) based on Zr-MOF (UiO-66) and CEA aptamer (Figure 6) [99]. In this work, CEA aptamer was used as the template to synthesize silver nanoclusters (AgNCs@Apt). The composite AgNCs@Apt @UiO-66 showed active electrochemical performance and high affinity toward CEA. When CEA was added, CEA aptamer can specifically bind with CEA, further resulting in the hinderance of redox probe to the surface of modified AE and the increase of R_{ct}. The proposed method has a wide linear range from 0.02 to 10 ng·mL^{-1} with a detection limit of 4.39 pg·mL^{-1}. Furthermore, the SPR aptasensor exhibits a higher detection limit of 0.3 ng·mL^{-1} within the CEA concentration of 1.0 ~ 250 ng·mL^{-1}. Gold nanoclusters (AuNCs) were also embedded into Zr-MOF (MOF-521) in Zhang's group via a one-pot method [96]. The MOFs was applied to construct electrochemical aptasensor for the detection of cocaine. To improve the loading capacity of aptamers, they successfully encapsulated three kinds of aptamer strands into Zr-MOF (MOF-509) for detection of thrombin, kanamycin, and CEA [100].

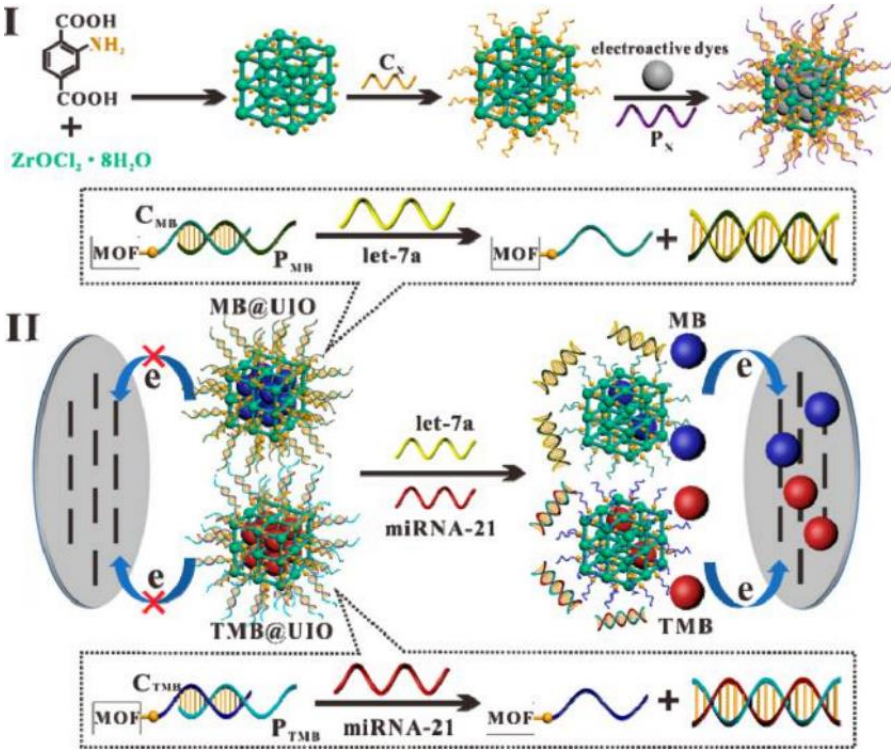

Figure 7. (I) Schematic representation of nucleic acid-functionalized MOFs fabrication procedure and (II) the principle of the MOF-based homogeneous electrochemical biosensor for multiple detection of miRNAs. Reprinted with permission from [101]. Copyright 2019 American Chemical Society.

Besides, due to the porous nanostructure, MOFs can also load electroactive dyes as nanocontainer with dsDNA as a gatekeeper to cap MOFs, which is released under certain stimulation. Li's group used dsDNA-capped UIO-66-NH_2 to load two electroactive dyes for ultrasensitive and simultaneous detection of let-7a and miRNA-21 (Figure 7) [101]. In this work, UIO-66-NH_2 was first prepared and linked with the carboxylated ssDNA C_X through the amidation reaction. Next, 3,3',5,5'-tetramethyl-benzidine (TMB) and methylene blue (MB) were entrapped into the pores of UIO-66-NH_2,

respectively. Then, another ssDNA P_X was used to partially hybridize with C_X and cap MOFs, which was completely complementary to the target biomarker. In the absence of target analytes, the dsDNA prevented the release of MB and TMB from MOFs, and no significant signal was detected. When target analytes were added, it was hybridized with P_X through the toehold-mediated strand-displacement reaction and moved away from MOFs, leading to the release of the corresponding entrapped dyes. The released MB and TMB produced two strong and typical peak currents.

Like the aforementioned aptasensors, in MOFs-based electrochemical immunosensor, the antibody-antigen interactions can result in an increase of the real component of impedance. In 2015, Deep's group reported an immunoassay for impedimetric sensing of parathion based on Cd-MOF and anti-parathion antibody [102]. Nanocomposites modified with redox species can be labeled with antibody for designing of amperometric immunosensors. For example, Yu's group synthesized a novel redox-active nanocomposite, AuPt-Methylene blue (MB) (AuPt-MB) [103]. The nanocomposite was applied to develop an amperometric biosensor for the determination of Galectin-3 (Gal-3).

In enzyme-based sensors, the immobilized enzyme can hydrolyze substrates into electroactive substances that can be oxidized or reduced on the surface of the electrocatalytic MOFs-modified electrode. Glucose oxidase (GOD) was immobilized on the surface of grapheme-metal coordination polymer composite nanosheet for the detection of glucose [104]. Chen and co-workers developed an efficient biosensing platform for bisphenol A (BPA) based on Cu-MOF and tyrosinase, in which Cu-MOF absorbed BPA through π–π stacking interactions and increased the available BPA concentration to react with tyrosinase [105]. Recently, Dong's group synthesized La-MOF-templated wool-ball-like carbon nanocomposites to immobilize acetylcholinesterase (AChE) for developing the enzyme biosensor for the detection of methyl parathion (Figure 8) [106]. In this work, three Fe^{3+}, Zr^{4+}, and La^{3+}-based MOFs were prepared with 2-aminoterephthalate (H_2ATA), and further were annealed at 550 °C under N_2 atmosphere. The MOFs-derived carbon materials not only possessed more active sites to immobilize AChE but also facilitated the electron transfer. AChE could hydrolyze into acetic acid and electroactive thiocholine (TCh), which was further electro-oxidized with the catalysis of the carbon nanocomposites on the surface of the electrode, generating irreversible oxidation peaks. Methyl parathion, a kind of pesticide, inhibited the catalytic activity of AChE and could be sensitively detected with a wide range and low detection limit.

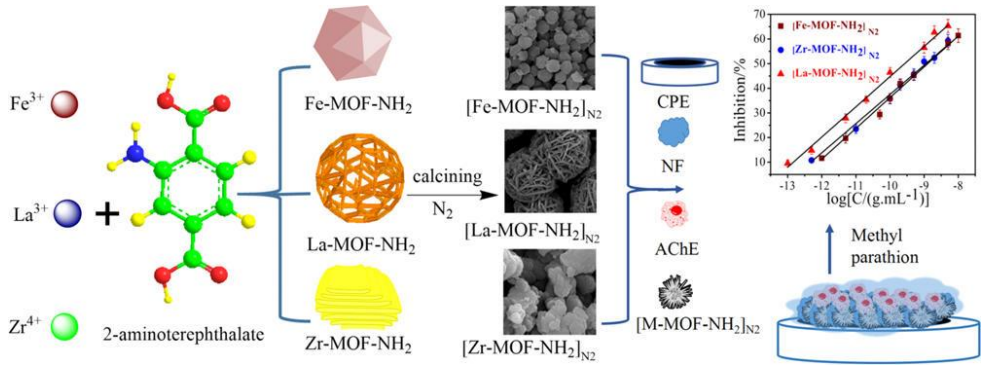

Figure 8. Schematic illustration of the fabrication processes of $[M\text{-}MOF\text{-}NH_2]_{N2}$ and detection of methyl parathion. Reprinted with permission from [106]. Copyright 2018 American Chemical Society.

4. CONCLUSION

As crystalline molecular materials, MOFs have many advantages over other nanomaterials, including chemical stability, tunable structure and property, and ultrahigh porosity. Significant progress has been achieved in the design of novel and excellent MOFs-based electrochemical sensors and biosensors in the past decade. However, further studies are still desired to address the shortcomings of MOFs, such as controllable synthesis in nanoscale dimension, higher conductivity and catalytic activity. With the achievements of nanoscience, MOFs-based electrochemical biosensors show very promising applications and the electrochemical-related researches will experience flourishing growth in the next few years.

ACKOWLEDGMENTS
Partial support of this work by the Anyang Normal University Program AYNUKP-2018-B20 and AYNUKP-2017-B16 was acknowledged.

References

1. J. Liu, L. Chen, H. Cui, J. Zhang, L. Zhang and C. Y. Su, *Chem. Soc. Rev.*, 43 (2014) 6011.
2. K. Lu, T. Aung, N. Guo, R. Weichselbaum and W. Lin, *Adv. Mater.*, 30 (2018) e1707634.
3. L. Liu, Y. Hao, D. Deng and N. Xia, *Nanomaterials*, 9 (2019) 316.
4. J. Lei, R. Qian, P. Ling, L. Cui and H. Ju, *TrAC-Trend. Anal.Chem.*, 58 (2014) 71.
5. L. Liu, D. Deng, W. Sun, X. Yang, S. Yang and S. He, *Int. J. Electrochem. Sci.*, 13 (2018) 10496.
6. C. Wang, J. Gao and H. Tan, *ACS Appl. Mater. Interfaces*, 10 (2018) 25113.
7. C. M. Doherty, D. Buso, A. J. Hill, S. Furukawa, S. Kitagawa and P. Falcaro, *Acc Chem. Res.*, 47 (2014) 396.
8. C. Zhang, M. Wang, L. Liu, X. Yang and X. Xu, *Electrochem. Commun.*, 33 (2013) 131.
9. L. Yang, C. Xu, W. Ye and W. Liu, *Sens. Actuat. B: Chem.*, 215 (2015) 489.
10. N. S. Lopa, M. M. Rahman, F. Ahmed, S. Chandra Sutradhar, T. Ryu and W. Kim, *Electrochim. Acta*, 274 (2018) 49.
11. B. Sherino, S. Mohamad, S. N. Abdul Halim and N. S. Abdul Manan, *Sens. Actuat. B: Chem.*, 254 (2018) 1148.
12. Y. Zhang, X. Bo, C. Luhana, H. Wang, M. Li and L. Guo, *Chem. Commun.*, 49 (2013) 6885.
13. E. Zhou, Y. Zhang, Y. Li and X. He, *Electroanalysis*, 26 (2014) 2526.
14. Z. Xu, L. Yang and C. Xu, *Anal. Chem.*, 87 (2015) 3438.
15. C. Li, T. Zhang, J. Zhao, H. Liu, B. Zheng, Y. Gu, X. Yan, Y. Li, N. Lu, Z. Zhang and G. Feng, *ACS Appl. Mater. Interfaces*, 9 (2017) 2984.
16. C. Zhang, X. Wang, M. Hou, X. Li, X. Wu and J. Ge, *ACS Appl. Mater. Interfaces*, 9 (2017) 13831.
17. W. Wei, S. Dong, G. Huang, Q. Xie and T. Huang, *Sens. Actuat. B: Chem.*, 260 (2018) 189.
18. C.-W. Kung, T.-H. Chang, L.-Y. Chou, J. T. Hupp, O. K. Farha and K.-C. Ho, *Electrochem. Commun.*, 58 (2015) 51.
19. A. T. Ezhil Vilian, B. Dinesh, R. Muruganantham, S. R. Choe, S.-M. Kang, Y. S. Huh and Y.-K. Han, *Microchim. Acta*, 184 (2017) 4793.
20. Y. Wang, Y. Wu, J. Xie and X. Hu, *Sens. Actuat. B: Chem.*, 177 (2013) 1161.

21. J. C. Jin, J. Wu, G. P. Yang, Y. L. Wu and Y. Y. Wang, *Chem. Commun.*, 52 (2016) 8475.
22. H. Guo, Z. Zheng, Y. Zhang, H. Lin and Q. Xu, *Sens. Actuat. B: Chem.*, 248 (2017) 430.
23. M. Lu, Y. Deng, Y. Luo, J. Lv, T. Li, J. Xu, S. W. Chen and J. Wang, *Anal. Chem.*, 91 (2018) 888.
24. W. Ma, Q. Jiang, P. Yu, L. Yang and L. Mao, *Anal. Chem.*, 85 (2013) 7550.
25. P. Ling, Q. Hao, J. Lei and H. Ju, *J. Mater. Chem. B*, 3 (2015) 1335.
26. S. Dong, D. Zhang, G. Suo, W. Wei and T. Huang, *Anal. Chim. Acta*, 934 (2016) 203.
27. Y. Shu, Y. Yan, J. Chen, Q. Xu, H. Pang and X. Hu, *ACS Appl. Mater. Interfaces*, 9 (2017) 22342.
28. X. Xiao, S. Zheng, X. Li, G. Zhang, X. Guo, H. Xue and H. Pang, *J. Mater. Chem. B*, 5 (2017) 5234.
29. W. Meng, Y. Wen, L. Dai, Z. He and L. Wang, *Sens. Actuat. B: Chem.*, 260 (2018) 852.
30. S. Shahrokhian, E. Khaki Sanati and H. Hosseini, *Biosens. Bioelectron.*, 112 (2018) 100.
31. Y. Zhang, J. Xu, J. Xia, F. Zhang and Z. Wang, *ACS Appl. Mater. Interfaces*, 10 (2018) 39151.
32. Y. Li, M. Xie, X. Zhang, Q. Liu, D. Lin, C. Xu, F. Xie and X. Sun, *Sens. Actuat. B: Chem.*, 278 (2019) 126.
33. W. Li, S. Lv, Y. Wang, L. Zhang and X. Cui, *Sens. Actuat. B: Chem.*, 281 (2019) 652.
34. Z. Chang, N. Gao, Y. Li and X. He, *Anal. Methods*, 4 (2012) 4037.
35. X. Wang, Q. Wang, Q. Wang, F. Gao, F. Gao, Y. Yang and H. Guo, *ACS Appl. Mater. Interfaces*, 6 (2014) 11573.
36. Y. Li, C. Huangfu, H. Du, W. Liu, Y. Li and J. Ye, *J. Electroanal. Chem.*, 709 (2013) 65.
37. Y. Wang, H. Ge, G. Ye, H. Chen and X. Hu, *J. Mater. Chem. B*, 3 (2015) 3747.
38. M. Q. Wang, C. Ye, S. J. Bao, Y. Zhang, Y. N. Yu and M. W. Xu, *Analyst*, 141 (2016) 1279.
39. Y.-Y. Zheng, C.-X. Li, X.-T. Ding, Q. Yang, Y.-M. Qi, H.-M. Zhang and L.-T. Qu, *Chin. Chem. Lett.*, 28 (2017) 1473.
40. X. Q. Wu, J. G. Ma, H. Li, D. M. Chen, W. Gu, G. M. Yang and P. Cheng, *Chem. Commun.*, 51 (2015) 9161.
41. H. Hosseini, H. Ahmar, A. Dehghani, A. Bagheri, A. R. Fakhari and M. M. Amini, *Electrochim. Acta*, 88 (2013) 301.
42. H. Hosseini, H. Ahmar, A. Dehghani, A. Bagheri, A. Tadjarodi and A. R. Fakhari, *Biosens. Bioelectron.*, 42 (2013) 426.
43. J. Zhou, X. Li, L. Yang, S. Yan, M. Wang, D. Cheng, Q. Chen, Y. Dong, P. Liu, W. Cai and C. Zhang, *Anal. Chim. Acta*, 899 (2015) 57.
44. S. Dong, G. Suo, N. Li, Z. Chen, L. Peng, Y. Fu, Q. Yang and T. Huang, *Sens. Actuat. B: Chem.*, 222 (2016) 972.
45. Y. Wang, L. Wang, H. Chen, X. Hu and S. Ma, *ACS Appl. Mater. Interfaces*, 8 (2016) 18173.
46. T. Q. N. Tran, G. Das and H. H. Yoon, *Sens. Actuat. B: Chem.*, 243 (2017) 78.
47. Y. Wang, W. Cao, L. Wang, Q. Zhuang and Y. Ni, *Microchim. Acta*, 185 (2018) 315.
48. J. Zhang, X. Xu and L. Chen, *Sens. Actuat. B: Chem.*, 261 (2018) 425.
49. L. Zhang and J. Zhang, *Biosens. Bioelectron.*, 110 (2018) 218.
50. J. Collman, X. Zhang, V. Lee, E. Uffelman and J. Brauman, *Science*, 261 (1993) 1404.
51. D. H. Lee, S. Kim, M. Y. Hyun, J. Y. Hong, S. Huh, C. Kim and S. J. Lee, *Chem. Commun.*, 48 (2012) 5512.
52. N. Xia, Y. Zhang, P. Guan, Y. Hao and L. Liu, *Sens. Actuators B: Chem.*, 213 (2015) 111.
53. H. L. Jiang, D. Feng, K. Wang, Z. Y. Gu, Z. Wei, Y. P. Chen and H. C. Zhou, *J. Am. Chem. Soc.*, 135 (2013) 13934.
54. J. W. Zhang, H. T. Zhang, Z. Y. Du, X. Wang, S. H. Yu and H. L. Jiang, *Chem. Commun.*, 50 (2014) 1092.
55. P. Ling, J. Lei, L. Zhang and H. Ju, *Anal. Chem.*, 87 (2015) 3957.
56. P. Ling, J. Lei and H. Ju, *Anal. Chem.*, 88 (2016) 10680.

57. P. Ling, J. Lei and H. Ju, *Biosens. Bioelectron.*, 71 (2015) 373.
58. L. Cui, J. Wu, J. Li and H. Ju, *Anal. Chem.*, 87 (2015) 10635.
59. W. J. Shen, Y. Zhuo, Y. Q. Chai and R. Yuan, *Anal. Chem.*, 87 (2015) 11345.
60. Z. Wang, H. Yu, J. Han, G. Xie and S. Chen, *Chem. Commun.*, 53 (2017) 9926.
61. H. Yu, J. Han, S. An, G. Xie and S. Chen, *Biosens. Bioelectron.*, 109 (2018) 63.
62. H. Wu, M. Li, Z. Wang, H. Yu, J. Han, G. Xie and S. Chen, *Anal. Chim. Acta*, 1049 (2019) 74.
63. W. Xu, Z. Qin, Y. Hao, Q. He, S. Chen, Z. Zhang, D. Peng, H. Wen, J. Chen, J. Qiu and C. Li, *Biosens. Bioelectron.*, 113 (2018) 148.
64. X. Yang, J. Lv, Z. Yang, R. Yuan and Y. Chai, *Anal. Chem.*, 89 (2017) 11636.
65. J. Chen, C. Yu, Y. Zhao, Y. Niu, L. Zhang, Y. Yu, J. Wu and J. He, *Biosens. Bioelectron.*, 91 (2017) 892.
66. T. Yan, L. Zhu, H. Ju and J. Lei, *Anal. Chem.*, 90 (2018) 14493.
67. N. Li, X. Huang, D. Sun, W. Yu, W. Tan, Z. Luo and Z. Chen, *Microchim. Acta*, 185 (2018) 543.
68. Y. Li, J. Jin, D. Wang, J. Lv, K. Hou, Y. Liu, C. Chen and Z. Tang, *Nano Res.*, 11 (2018) 3294.
69. C. Wang, G. Sudlow, Z. Wang, S. Cao, Q. Jiang, A. Neiner, J. J. Morrissey, E. D. Kharasch, S. Achilefu and S. Singamaneni, *Adv Healthc Mater*, 7 (2018) e1800950.
70. X. Yang, Q. Tang, Y. Jiang, M. Zhang, M. Wang and L. Mao, *J. Am. Chem. Soc.*, 141 (2019) 3782.
71. C. Liu, J. Dong, S. Ning, J. Hou, G. I. N. Waterhouse, Z. Cheng and S. Ai, *Microchim. Acta*, 185 (2018) 423.
72. D. Zhao, T. Wang, D. Han, C. Rusinek, A. J. Steckl and W. R. Heineman, *Anal. Chem.*, 87 (2015) 9315.
73. X. Dai, F. Qiu, X. Zhou, Y. Long, W. Li and Y. Tu, *Anal. Chim. Acta*, 848 (2014) 25.
74. Y. Shahbazi, F. Ahmadi and F. Fakhari, *Food Chem.*, 192 (2016) 1060.
75. Y. Lin, Q. Zhou, J. Li, J. Shu, Z. Qiu, Y. Lin and D. Tang, *Anal. Chem.*, 88 (2016) 1030.
76. N. Xia, L. Liu, Y. Chang, Y. Hao and X. Wang, *Electrochem. Commun.*, 74 (2017) 28.
77. N. Xia, X. Wang, B. Zhou, Y. Wu, W. Mao and L. Liu, *ACS Appl. Mater. Interfaces*, 8 (2016) 19303.
78. N. Xia, Z. H. Chen, Y. D. Liu, H. Z. Ren and L. Liu, *Sens. Actuat. B: Chem.*, 243 (2017) 784.
79. N. Xia, P. Peng, S. Wang, J. Du, G. Zhu, W. Du and L. Liu, *Sens. Actuat. B: Chem.*, 232 (2016) 557.
80. L. Liu, C. Cheng, Y. Chang, H. Ma and Y. Hao, *Sens. Actuat. B: Chem.*, 248 (2017) 178.
81. D. Deng, Y. Hao, S. Yang, Q. Han, L. Liu, Y. Xiang, F. Tu and N. Xia, *Sens. Actuat. B: Chem.*, 286 (2019) 415.
82. D. Deng, L. Liu, Y. Bu, X. Liu, X. Wang and B. Zhang, *Sens. Actuat. B: Chem.*, 269 (2018) 189.
83. L. N. Feng, Z. P. Bian, J. Peng, F. Jiang, G. H. Yang, Y. D. Zhu, D. Yang, L. P. Jiang and J. J. Zhu, *Anal. Chem.*, 84 (2012) 7810.
84. F. F. Cheng, T. T. He, H. T. Miao, J. J. Shi, L. P. Jiang and J. J. Zhu, *ACS Appl. Mater. Interfaces*, 7 (2015) 2979.
85. H. Gao, X. Jiang, Y. J. Dong, W. X. Tang, C. Hou and N. N. Zhu, *Biosens. Bioelectron.*, 48 (2013) 210.
86. M. Chen, N. Gan, Y. Zhou, T. Li, Q. Xu, Y. Cao and Y. Chen, *Sens. Actuat. B: Chem.*, 242 (2017) 1201.
87. Y. Yang, J. Cheng, B. Wang, Y. Guo, X. Dong and J. Zhao, *Microchim. Acta*, 186 (2019) 101.
88. T. Z. Liu, R. Hu, X. Zhang, K. L. Zhang, Y. Liu, X. B. Zhang, R. Y. Bai, D. Li and Y. H. Yang, *Anal. Chem.*, 88 (2016) 12516.
89. P. Zhang, H. Huang, N. Wang, H. Li, D. Shen and H. Ma, *Microchim. Acta*, 184 (2017) 4037.
90. L. Liu, Y. Chang, J. Yu, M. Jiang and N. Xia, *Sens. Actuat. B: Chem.*, 251 (2017) 359.
91. L. Liu, D. H. Deng, Y. Wang, K. Song, Z. Shang, Q. Wang, N. Xia and B. Zhang, *Sens. Actuat. B: Chem.*, 266 (2018) 246.

92. N. Xia, B. Zhou, N. Huang, M. Jiang, J. Zhang and L. Liu, *Biosens. Bioelectron.*, 85 (2016) 625.
93. G. Y. Zhang, S. Y. Deng, W. R. Cai, S. Cosnier, X. J. Zhang and D. Shan, *Anal. Chem.*, 87 (2015) 9093.
94. G. Y. Zhang, C. Cai, S. Cosnier, H. B. Zeng, X. J. Zhang and D. Shan, *Nanoscale*, 8 (2016) 11649.
95. X. Liu, M. Hu, M. Wang, Y. Song, N. Zhou, L. He and Z. Zhang, *Biosens. Bioelectron.*, 123 (2019) 59.
96. F. Su, S. Zhang, H. Ji, H. Zhao, J. Y. Tian, C. S. Liu, Z. Zhang, S. Fang, X. Zhu and M. Du, *ACS Sens.*, 2 (2017) 998.
97. Z. Zhang, H. Ji, Y. Song, S. Zhang, M. Wang, C. Jia, J. Y. Tian, L. He, X. Zhang and C. S. Liu, *Biosens. Bioelectron.*, 94 (2017) 358.
98. C. S. Liu, Z. H. Zhang, M. Chen, H. Zhao, F. H. Duan, D. M. Chen, M. H. Wang, S. Zhang and M. Du, *Chem. Commun.*, 53 (2017) 3941.
99. C. Guo, F. Su, Y. Song, B. Hu, M. Wang, L. He, D. Peng and Z. Zhang, *ACS Appl. Mater. Interfaces*, 9 (2017) 41188.
100. Z. H. Zhang, F. H. Duan, J. Y. Tian, J. Y. He, L. Y. Yang, H. Zhao, S. Zhang, C. S. Liu, L. H. He, M. Chen, D. M. Chen and M. Du, *ACS Sens.*, 2 (2017) 982.
101. J. Chang, X. Wang, J. Wang, H. Li and F. Li, *Anal. Chem.*, 91 (2019) 3604.
102. A. Deep, S. K. Bhardwaj, A. K. Paul, K. H. Kim and P. Kumar, *Biosens. Bioelectron.*, 65 (2015) 226.
103. Z. Tang, J. He, J. Chen, Y. Niu, Y. Zhao, Y. Zhang and C. Yu, *Biosens. Bioelectron.*, 101 (2018) 253.
104. Y. Guo, Y. Han, S. Shuang and C. Dong, *J. Mater. Chem.*, 22 (2012) 13166.
105. X. Wang, X. Lu, L. Wu and J. Chen, *Biosens. Bioelectron.*, 65 (2015) 295.
106. S. Dong, L. Peng, W. Wei and T. Huang, *ACS Appl. Mater. Interfaces*, 10 (2018) 14665.